Contents lists available at ScienceDirect

Arthroplasty Today

Original Research

Primary Stability of Collared and Collarless Cementless Femoral Stems — A Finite Element Analysis Study

Ryunosuke Watanabe, MD, Hajime Mishima, MD, PhD [*], Sho Totsuka, MD, Tomofumi Nishino, MD, PhD, Masashi Yamazaki, MD, PhD

Department of Orthopaedic Surgery, Institute of Medicine, University of Tsukuba, Tsukuba, Japan

A B S T R A C T

Background: Primary stability of the femoral stem is important for the long-term results of cementless total hip arthroplasty. Cementless collared stems have been known to have higher stability than collarless stems when there is a contact between the collar and the calcar. The purpose of this study was to compare the stabilities of collared stem and collarless stem in 2 loading conditions: 1) flat walking and 2) stair climbing.
Methods: We constructed 3 finite element models. In the first model, the collar had contact with the calcar. The second model had a 1 mm gap between the calcar and the collar. The third model was constructed with a collarless stem. The proximal femur around the stem was divided into 3 zones: the upper zone (Gruen zones 1 and 7), the middle zone (Gruen zones 2 and 6), and the lower zone (Gruen zones 3 and 5). The micromotion at the stem/bone interface was measured at each zone of the 3 models under the 2 loading conditions.
Results: The results showed that collared stems were more stable when the collar was in contact with the calcar than when a gap was left between the collar and the calcar. In particular, collar contact was highly effective in suppressing the micromotion proximal to the stem.
Conclusions: Compared to the collarless stem, the collared stem had comparable stability when there was a gap at the collar and calcar interface and higher stability when there was contact between the collar and the calcar.
© 2023 The Authors. Published by Elsevier Inc. on behalf of The American Association of Hip and Knee Surgeons. This is an open access article under the CC BY-NC-ND license (http://creativecommons.org/licenses/by-nc-nd/4.0/).

Introduction

Total hip arthroplasty (THA) is a standard orthopedic procedure for the treatment of deformed hip joints, which alleviates pain and improves function. THA is performed worldwide, and good long-term results have been reported owing to recent improvements in implants and surgical techniques. However, problems such as aseptic loosening, bone atrophy, infection, dislocation, and periprosthetic fractures after THA surgery remain, which affect the long-term results [1].

There are various designs and types of cementless stems, each of which has been reported to yield good long-term results [2]. The success of cementless stems requires good initial fixation to achieve bone growth and osseointegration at the coated surface of the stem [3,4]. The initial fixation of cementless stems is achieved by the mechanical stability between the stem and the bone. In the early postoperative period after THA, loading causes micromotion (MM) of less than 1 mm between the stem and bone, which is defined as MM. MMs larger than 150 μm were reported to inhibit osseointegration due to the formation of fibrous tissue between the stem and bone [3,5,6].

This study aimed to investigate the effect of the cementless stem collar on stem stability when a gap is left between the collar and the cut surface of the medial calcar using finite element analysis (FEA).

Material and methods

Materials

The composite femur used in this study (composite femur#3403, Pacific Research Laboratories, USA) was manufactured from glass-filled epoxy. It is made to mimic the mechanical

* Corresponding author. Department of Orthopaedic Surgery, Institute of Medicine, University of Tsukuba, 1-1-1 Tennodai, Tsukuba 305-8575, Japan. Tel.: +81 29853 3219.
E-mail address: hmishima@md.tsukuba.ac.jp

properties and morphology of natural human bone based on male patients' data and is composed of cortical and cancellous bone [7,8]. We used the Universia stem (Teijin Nakashima Medical, Japan), which is one of the fully hydroxyapatite (HA)-coated stems. This stem has been in use in Japan since 2020. It is a collared stem made of titanium alloy (Ti-6Al-4V) with a 150 μm HA coating on the surface. We used computer-aided design (CAD) data from a collared Universia stem and a collarless stem with the same shape as the collared stem for the finite element analysis. CAD data was provided by Teijin Nakashima Medical.

Methods

Computed tomography (CT) scans (Supria, Q2J-BW1645-1; Hitachi Medical Corporation, Japan) were performed with a bone mass phantom (QRM-BDC, QRM, Germany) and saved as digital imaging and communications in medicine data. The following scanner settings were employed: 1.25 mm slice thickness, 1 mm slice spacing, 20 cm field of view, and 512 × 512 pixel resolution.

We used the Mechanical Finder ver 11.0 (Research Center of Computational Mechanics, Japan) to create and analyze the finite element model.

The stem was aligned to the proximal femoral shaft axis of the composite femur. We chose the largest stem size that would fit the proximal medullary canal geometry. Stem depth and offset were determined so that the neck center reproduced the center of the simulated femoral head. For these reasons, CAD data of the high-offset collared stem and collarless stem of Universia stem#11 were used.

Three finite-element models were constructed. The "contact model (C)" was in contact with the cut surface of the medial calcar and stem collar. The "non-contact model (NC)" had the same stem position as the "contact model", but the cut surface was lowered 1 mm to avoid contact between the collar and cut surface. The "collarless model (CL)" used a collarless stem and had the same stem position as the "contact model" (Fig. 1).

We used 1- to 4-mm 4-node tetrahedral solid elements to construct a three-dimensional (3D) finite element model for the composite femur, and triangular plate shell elements with a thickness of 0.001 mm were attached to the synthetic femoral surface. We used 0.5- to 2-mm 4-node tetrahedral solid elements to construct a 3D finite element model for the stem. The finite element model of the synthetic femur and stem consisted of approximately 220,000 nodes, 1,100,000 elements, and 45,000 shells. The Young's modulus of the synthetic femur was determined using the equations proposed by Keyak et al. according to CT density values [9]. Poisson's ratio of the synthetic femur was assumed to be 0.4. The Young's modulus and Poisson's ratio of the stem were set to 108 GPa and 0.28, respectively, based on the material property values of Ti-6Al-4V. A coefficient of friction of 0.6 was set between the stem and the composite femur [10,11]. Joint contact and muscle forces were simulated as peak forces in flat walking and stair climbing, which exert the greatest rotational force in daily life (Fig. 2a and b). For the flat walking condition, the joint reaction force travels through the trunnion center, and the tensile load is applied to the greater trochanter by the abductors and tensor fascia latae and to the lateral side of the femur by the vastus lateralis. In the stair climbing condition, the joint reaction force travels through the trunnion center, and the tensile load is applied to the greater trochanter by the abductors, tensor fascia latae, and iliotibial tract, to the lateral side of the femur by the vastus lateralis, and to the medial side of the femur by the vastus medialis muscles [12]. For both loading conditions, a body weight of 60 kg was assumed. The femoral condyle was fixed. The relative displacement between the stem nodes and the bone contact surface is defined as the MM [13]. The median MM values of the 3 finite element models were compared for the flat walking and stair-climbing conditions. Gruen zones 1 and 7 were set as the upper zone of the stem, zones 2 and 6 as the middle zone, and zones 3 and 5 as the lower zone; the MM for each of the 3 zones was compared between the 3 models under the 2 loading conditions [14]. A contour diagram of the 3D model was created to evaluate the MM of the entire stem.

Statistical analyses were performed using SPSS version 29 (IBM, USA). MMs of the 3 models were compared using the Kruskal−Wallis test followed by the Dunn test for each of the 2 loading conditions. *P*-value was set at $P < .05$.

Results

In both the flat walking and stair climbing conditions, the mean MM of the contact model was significantly smaller than that of the noncontact and collarless models ($P < .01$) (Fig. 3a and b). The mean MM at each zone according to the type of stem under flat walking conditions was C: 94 μm, NC: 115 μm, CL: 115 μm in the upper zone, C: 45 μm, NC: 54 μm, CL: 55 μm in the middle zone, C: 113 μm, NC: 117 μm, CL: 118 μm in the lower zone. For each zone of flat walking
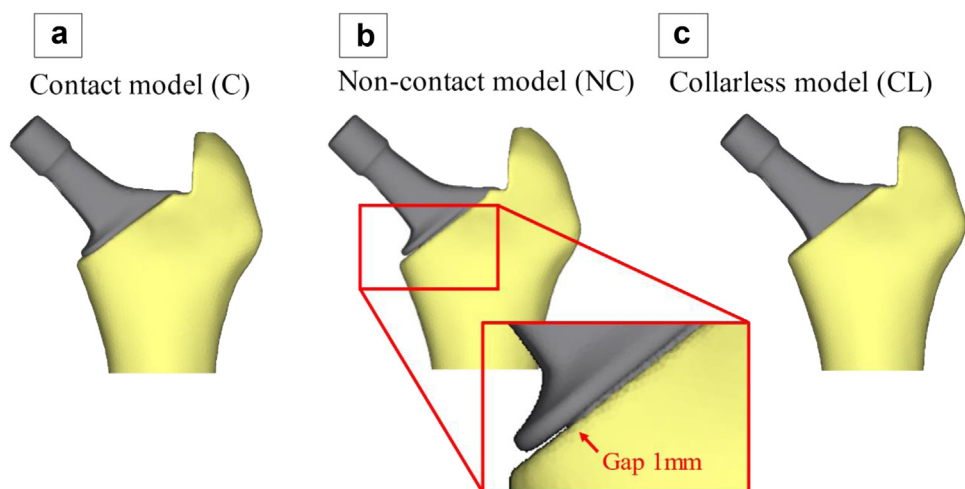

Figure 1. Three finite element models. (a) The "contact model" was in contact with the cut surface of the medial calcar and stem collar. (b) The "non-contact model" had a 1 mm gap between the calcar and collar. (c) The "collarless model" used a collarless stem and had the same stem position as the "contact model".
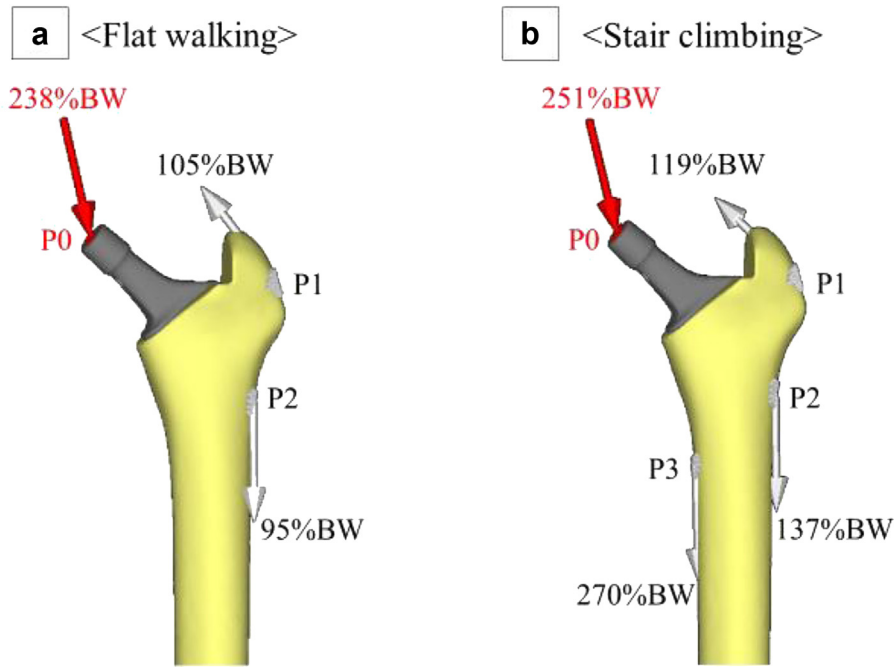
Figure 2. Two loading conditions are applied to each model. (a) The loads applied during flat walking simulations include the hip joint contact force through the trunnion center (P0), the tensile force of the abductors and tensor fascia latae at P1, and the tensile force of the vastus lateralis at P2. (b) The loads applied during stair climbing simulations include the hip joint contact force through the trunnion center (P0), the tensile force of the abductors, tensor fascia latae, and iliotibial tract at P1, the tensile force of the vastus lateralis at P2, and the tensile force of the vastus medialis at P3. For both conditions, body weight (BW) was assumed to be 60 kg.

condition, the contact model had a significantly smaller MM than did the non-contact model and the collarless model in all zones ($P <$ .01) (Fig. 4a-c). In addition, the mean MM at each zone according to the type of stem under stair climbing condition was C: 134 μm, NC: 166 μm, CL: 166 μm in the upper zone, C: 66 μm, NC: 77 μm, CL: 79 μm in the middle zone, C: 160 μm, NC: 165 μm, CL: 168 μm in the lower zone. For each zone of the stair climbing condition, the contact model had a significantly smaller MM than did the non-contact model and the collarless model in the upper zone and middle zone ($P <$ .01). Moreover, the contact model had a significantly smaller MM than did the collarless model in the lower zone ($P <$ .01). There was also a significant difference between the non-contact and collarless models in the upper zone ($P <$ .05) (Fig. 4d-f).

The median MM of the contact and collarless models for flat walking conditions in each zone showed that the contact model was 25% smaller than the collarless model in the upper zone, 18% smaller in the middle zone, and 9% smaller in the lower zone. Similarly, the median MM of the contact model and collarless model for the stair climbing condition for each zone showed that the contact model was 26% smaller than the collarless model in the upper zone but 20% smaller in the middle zone and 7% smaller in the lower zone.

Contour diagrams of the MM for the 3 models in the flat walking and stair climbing conditions are shown in Figures 5 and 6. In the flat walking condition, the red zones (MM > 150 μm) were concentrated on the anterior and posterior surfaces of the upper
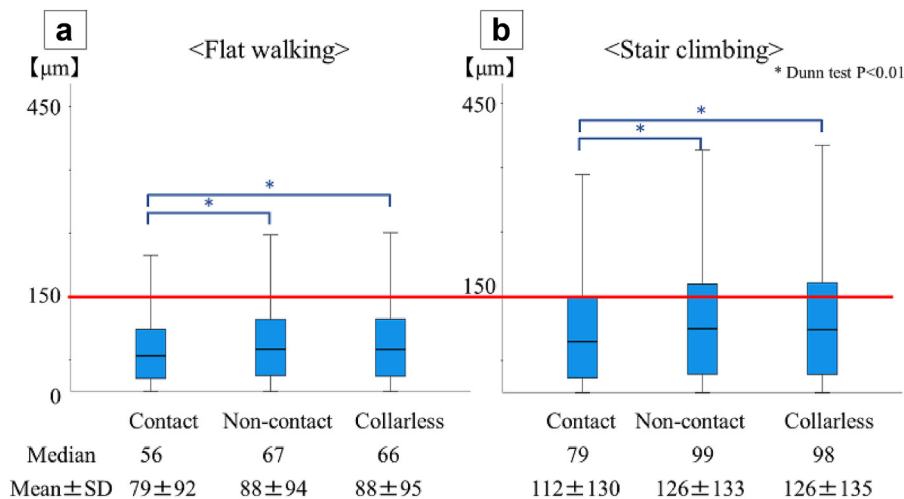

Figure 3. Comparison of micromotion among 3 finite element models under (a) flat walking and (b) stair-climbing conditions. The micromotion of the contact model was significantly smaller than that of the noncontact and collarless models under both loading conditions. SD, standard deviation.
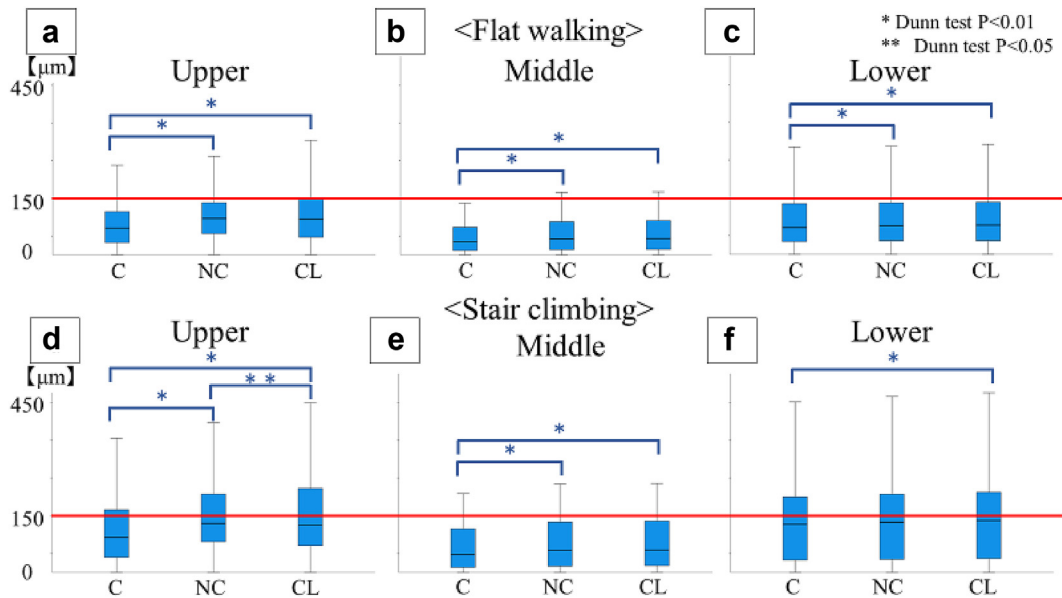
Figure 4. Comparison of micromotion between 3 zones of the stem (upper, middle, and lower) among 3 finite element models under 2 loading conditions. a-c showed micromotion under flat walking conditions. d-f showed micromotion under stair climbing. The micromotion of the contact model was significantly smaller than the non-contact model and collarless model in all zones. C, contact model; NC, non-contact model; Cl, collarless model.

zone and at the tip of the stem. In the non-contact and collarless models, the red zones were wider than those in the contact model on the anterior and posterior surfaces near the collar and on the lateral surface of the stem (Fig. 5). In the contour diagram of the 3 models for the stair climbing condition, the red zones were spread over a wider area than in the flat walking condition (Fig. 6). The percentage of nodes with MM greater than 150 μm was shown in Table 1. In both loading conditions, nodes with MM greater than 150 μm were concentrated in the upper and lower zones.

Discussion

In this study, the effect of the collar of a cementless stem on the stability of the stem was evaluated using FEA. MM was evaluated by

FEA using digital imaging and communications in medicine data of a composite femur and CAD data of the Universia stem, which is one of the fully HA-coated stems. The MM of the collared stem was found to be smaller and more stable than that of the collarless stem under flat walking and stair climbing conditions. The stability of the proximal portion of the stem was increased by the collar. The collar provided stability when in contact with the cut surface of the medial calcar and was as stable as the collarless stem when not in contact with the cut surface of the medial calcar.

A fully HA-coated stem is a cementless stem in which the entire surface of the stem is coated with HA. The Corail (Depuy Synthes, United States of America) was first used in 1986, and other stems have since been launched and reported to have good results [15,16]. However, there have been a few reports of early postoperative stem
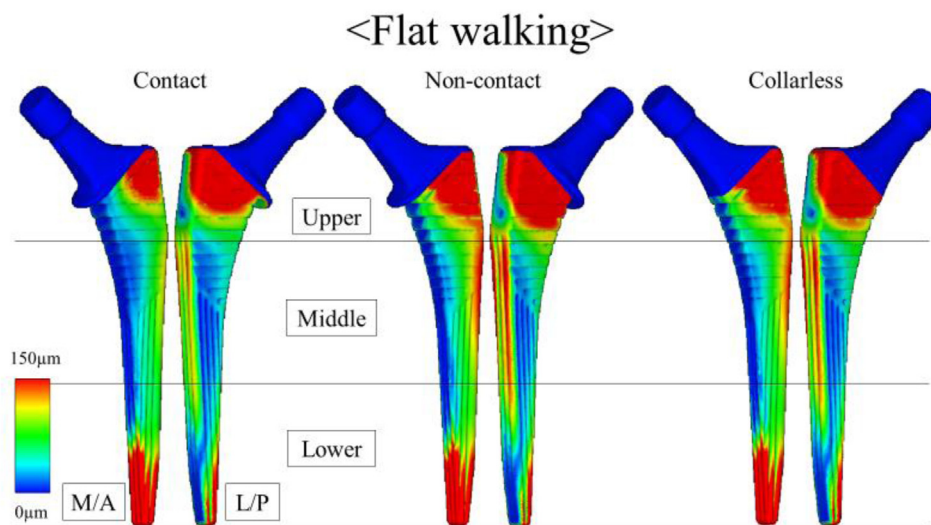

Figure 5. The distribution of micromotion of 3 finite element models under flat walking condition. The left model showed medial and anterior aspects of the stem, and the right model showed lateral and posterior aspects of the stem. In all models, red zones (micromotion >150 μm) were concentrated on the anterior and posterior aspects of the upper zone and at the tip of the stem. More red zones were observed on the anterior and posterior aspects near the collar and the lateral aspect of the stem than in the contact model.
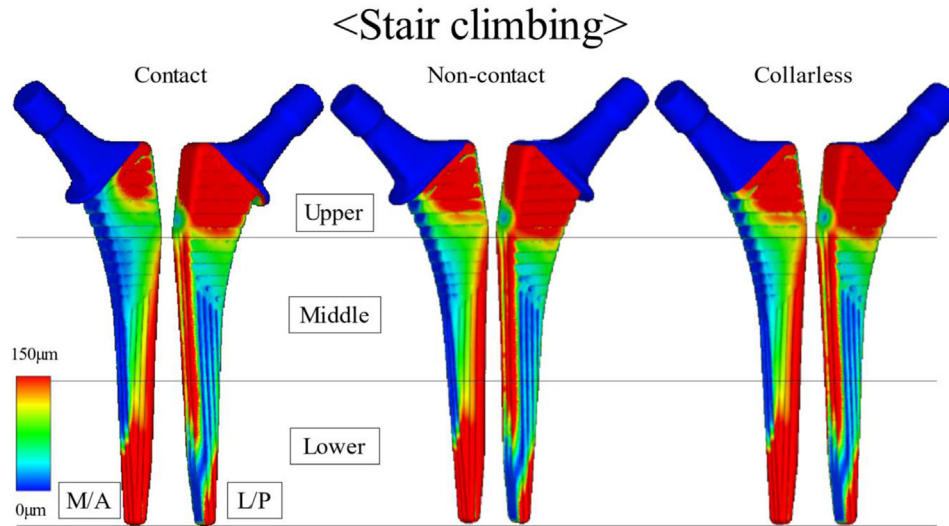
Figure 6. The distribution of micromotion of 3 finite element models under stair climbing conditions. The left model showed the medial and anterior aspects of the stem, and the right model showed the lateral and posterior aspects of the stem. In all models, red zones (micromotion >150 μm) were concentrated on the anterior and posterior aspects of the upper zone, the lateral aspect of the middle zone, and at the tip of the stem.

subsidence for the collarless type of Corail, and the use of collared type is now recommended [17,18].

Comparisons between collared and collarless stems have long been reported in mechanical experiments using cadaveric and simulated bones as well as in FEA. Collared stems have been reported to have higher vertical and rotational stabilities than collarless stems [19,20]. Mechanical experiments have also revealed that collared stems are more resistant to periprosthetic fractures [21,22]. According to registry data, collarless stems have a higher risk of periprosthetic fracture in the early postoperative period than collared stems. It has also been suggested that the collar and medial calcar should be in contact or have a gap of 1 mm or less to increase the resistance to periprosthetic fractures [23]. However, there are no reports that we have been able to find on the effect of a gap between the collar and medial calcar on stem primary stability.

Past finite element analyses found that collared stems suppressed MM better than collarless stem [10,20]. However, the difference in the median MM between the collared and collarless stems was small, so the difference would not clinically affect the stability of the stems. Even when the collar of the collared stem did not make contact with the calcar, MM around the stem was equivalent to that of the collarless stem, and the stability was not significantly reduced. Although greater stability is achieved if the collar is in contact with the calcar, we believe that if the stem size is appropriate for the medullary canal, stability is likely to be acceptable even if the collar is not in contact with the calcar.

Table 1
The percentages of nodes with MM greater than 150 μm are shown in Table.

<Flat walking>	Total	Upper	Middle	Lower	
Contact	11	17	0	23	
Noncontact	13	22	2	23	
Collarless	14	25	2	23	[%]
<Stair climbing>	Total	Upper	Middle	Lower	
Contact	25	29	11	41	
Noncontact	32	41	20	44	
Collarless	32	38	20	45	[%]

In both loading conditions, nodes with MM greater than 150 μm were concentrated in the upper and lower zones.

Further study is needed when the stem is undersized for the medullary canal and the collar is in contact with calcar.

When MM greater than 150 μm occurs between the porous-coated portion of the cementless stem and the bone, bone growth is inhibited [3,5,6]. In this study, the median MM for the whole stem was less than 150 μm in both flat walking and stair climbing conditions, but there were areas greater than 150 μm in the upper and lower zones of the stem. Past studies have reported that MM was greater than the 95% value at the proximal and distal ends of the fully HA-coated stem type and short tapered-wedge stem type [10,24]. Additionally, the percentage of nodes greater than 150 μm in the contact model was only 11% in the flat walking condition and 25% in the stair-climbing condition. The Universia stem is coated with HA on the whole surface of the stem, and osseointegration between HA and the bone is expected. Therefore, even if MM increases in one part of the stem, there may be no problem with the stability of the entire stem. In the future, it will be necessary to observe the progress of patients using the Universia stem for THA to check for loosening of the stem and the appearance of radiolucent lines and compare the results with those of the present study.

In this study, 2 loading conditions were selected: flat walking and stair climbing. Both movements are performed in daily life, and stair climbing exerts the greatest rotation torque on the stem among daily life movements [12]. Evaluations of MM performed under similar loading conditions by FEA revealed that MM and strain around the stem were greater in the stair climbing condition than in the flat walking condition [10,25]. MM was greater in the stair climbing condition than in the flat walking condition in all 3 models (contact, non-contact, and collarless models) of our study, and we believe that this was an appropriate loading condition for the FEA.

This study had several limitations. The first limitation was the use of CT data from the composite femur, which may have affected the MM values because the composite femur did not have the same strength as the actual femur. The Universia stem also creates a layer of compressed cancellous bone around the stem by compaction rasp. In this study, the analysis was also performed with cancellous bone interposed between the stem and the cortical bone. However, the strength of the compressed cancellous bone was not reproduced by FEA. Therefore, it is possible that the stability of the stem

was decreasing and that of the MM was greater. Second, this study did not directly compare and verify the results of FEA with those of mechanical examinations.

Conclusions

Compared to the collarless stem, the collared stem had comparable stability when there was a gap at the collar and calcar interface and higher stability when there was contact between the collar and the calcar. However, the difference in MM was small and had little impact on the clinical outcome. It was found that the stability of a properly sized stem did not change significantly depending on whether the collar of the collared stem was in contact with the calcar.

Conflicts of interest

The authors declare there are no conflicts of interest.
For full disclosure statements refer to https://doi.org/10.1016/j.artd.2023.101140.

Acknowledgments

The authors thank Teijin Nakashima Medical for preparing the CAD data for the stem. Special thanks to Dr. Keita Uetsuki and Mr. Tsutomu Hochu for their support and helpful discussion.

References

[1] Pivec R, Johnson AJ, Mears SC, Mont MA. Hip arthroplasty. Lancet 2012;380: 1768—77. https://doi.org/10.1016/S0140-6736(12)60607-2.
[2] Khanuja HS, Vakil JJ, Goddard MS, Mont MA. Cementless femoral fixation in total hip arthroplasty. J Bone Joint Surg Am 2011;93:500—9. https://doi.org/10.2106/JBJS.J.00774.
[3] Pilliar RM, Lee JM, Maniatopoulos C. Observations on the effect of movement on bone ingrowth into porous-surfaced implants. Clin Orthop Relat Res 1986;208:108. https://doi.org/10.1097/00003086-198607000-00023.
[4] Søballe K, Toksvig-Larsen S, Gelineck J, Fruensgaard S, Hansen ES, Ryd L, et al. Migration of hydroxyapatite coated femoral prostheses. A Roentgen stereophotogrammetric study. J Bone Joint Surg Br 1993;75:681—7. https://doi.org/10.1302/0301-620X.75B5.8397213.
[5] Engh CA, O'Connor D, Jasty M, McGovern TF, Bobyn JD, Harris WH. Quantification of implant micromotion, strain shielding, and bone resorption with porous-coated anatomic medullary locking femoral prostheses. Clin Orthop Relat Res 1992;285:13—29. https://doi.org/10.1097/00003086-199212000-00005.
[6] Jasty M, Bragdon C, Burke D, O'Connor D, Lowenstein J, Harris WH. In vivo skeletal responses to porous-surfaced implants subjected to small induced motions. J Bone Joint Surg Am 1997;79:707—14. https://doi.org/10.2106/00004623-199705000-00010.
[7] Heiner AD, Brown TD. Structural properties of a new design of composite replicate femurs and tibias. J Biomech 2001;34:773—81. https://doi.org/10.1016/s0021-9290(01)00015-x.
[8] Heiner AD. Structural properties of fourth-generation composite femurs and tibias. J Biomech 2008;41:3282—4. https://doi.org/10.1016/j.jbiomech.2008.08.013.
[9] Keyak JH, Rossi SA, Jones KA, Skinner HB. Prediction of femoral fracture load using automated finite element modeling. J Biomech 1998;31:125—33. https://doi.org/10.1016/s0021-9290(97)00123-1.
[10] Al-Dirini RMA, Huff D, Zhang J, Besier T, Clement JG, Taylor M. Influence of collars on the primary stability of cementless femoral stems: a finite element study using a diverse patient cohort. J Orthop Res 2018;36:1185—95. https://doi.org/10.1002/jor.23744.
[11] Viceconti M, Muccini R, Bernakiewicz M, Baleani M, Cristofolini L. Large-sliding contact elements accurately predict levels of bone—implant micromotion relevant to osseointegration. J Biomech 2000;33:1611—8. https://doi.org/10.1016/S0021-9290(00)00140-8.
[12] Heller MO, Bergmann G, Kassi JP, Claes L, Haas NP, Duda GN. Determination of muscle loading at the hip joint for use in pre-clinical testing. J Biomech 2005;38:1155—63. https://doi.org/10.1016/j.jbiomech.2004.05.022.
[13] Pal B, Gupta S, Andrew MR, Browne M. Strain and micromotion in intact and resurfaced composite femurs: experimental and numerical investigations. J Biomech 2010;43:1923—30. https://doi.org/10.1016/j.jbiomech.2010.03.019.
[14] Gruen TA, Mcneice GM, Amstutz HC. 'Modes of Failure' of cemented stem-type femoral components: a radiographic analysis of loosening. Clin Orthop Relat Res 1979;141:17—27. https://doi.org/10.1097/00003086-197906000-00002.
[15] Cypres A, Fiquet A, Girardin P, Fitch D, Bauchu P, Bonnard O, et al. Long-term outcomes of a dual-mobility cup and cementless triple-taper femoral stem combination in total hip replacement: a multicenter retrospective analysis. J Orthop Surg Res 2019;14:376. https://doi.org/10.1186/s13018-019-1436-y.
[16] Vidalain JP. Twenty-year results of the cementless Corail stem. Int Orthop 2011;35:189—94. https://doi.org/10.1007/s00264-010-1117-2.
[17] Selvaratnam V, Shetty V, Sahni V. Subsidence in collarless Corail hip replacement. Open Orthop J 2015;9:194—7. https://doi.org/10.2174/1874325001509010194.
[18] Song JH, Jo WL, Lee KH, Cho YJ, Park J, Oh S. Subsidence and perioperative periprosthetic fractures using collarless hydroxyapatite-coated stem for displaced femoral neck fractures according to Dorr type. J Orthop Surg (Hong Kong) 2019;27. https://doi.org/10.1177/2309499019877530. 2309499019877530.
[19] Demey G, Fary C, Lustig S, Neyret P, si Selmi T. Does a collar improve the immediate stability of uncemented femoral hip stems in total hip arthroplasty? A bilateral comparative cadaver study. J Arthroplasty 2011;26: 1549—55. https://doi.org/10.1016/j.arth.2011.03.030.
[20] Keaveny TM, Bartel DL. Effects of porous coating, with and without collar support, on early relative motion for a cementless hip prosthesis. J Biomech 1993;26:1355—68. https://doi.org/10.1016/0021-9290(93)90087-U.
[21] Johnson AJ, Desai S, Zhang C, Koh K, Zhang LQ, Costales T, et al. A calcar collar is protective against early torsional/spiral periprosthetic femoral fracture: a paired cadaveric biomechanical analysis. J Bone Joint Surg Am 2020;102: 1427—33. https://doi.org/10.2106/JBJS.19.01125.
[22] Lamb JN, Baetz J, Messer-Hannemann P, Adekanmbi I, van Duren BH, Redmond A, et al. A calcar collar is protective against early periprosthetic femoral fracture around cementless femoral components in primary total hip arthroplasty: a registry study with biomechanical validation. Bone Joint J 2019;101—B:779—86. https://doi.org/10.1302/0301-620X.101B7.BJJ-2018-1422.R1.
[23] Lamb JN, Coltart O, Adekanmbi I, Pandit HG, Stewart T. Calcar-collar contact during simulated periprosthetic femoral fractures increases resistance to fracture and depends on the initial separation on implantation: a composite femur in vitro study. Clin Biomech (Bristol Avon) 2021;87:105411. https://doi.org/10.1016/j.clinbiomech.2021.105411.
[24] Kanaizumi A, Suzuki D, Nagoya S, Teramoto A, Yamashita T. Patient-specific three-dimensional evaluation of interface micromotion in two different short stem designs in cementless total hip arthroplasty: a finite element analysis. J Orthop Surg Res 2022;17:437. https://doi.org/10.1186/s13018-022-03329-5.
[25] Al-Dirini RMA, Martelli S, Huff D, Zhang J, Clement JG, Besier T, et al. Evaluating the primary stability of standard vs lateralised cementless femoral stems — a finite element study using a diverse patient cohort. Clin Biomech 2018;59: 101—9. https://doi.org/10.1016/j.clinbiomech.2018.09.002.